Pergamon

Cement and Concrete Research, Vol. 25, No. 2, pp. 319-331, 1995
Copyright © 1995 Elsevier Science Ltd
Printed in the USA. All rights reserved
0008-8846/95 $9.50+.00

0008-8846(95)00017-8

NUMERICAL SIMULATION OF HYDRATION AND MICROSTRUCTURAL DEVELOPMENT IN HARDENING CEMENT-BASED MATERIALS
(I) Theory

K. van Breugel
Technical University of Technology
Delft, The Netherlands

(Refereed)
(Received July 28, 1992; in final form November 7, 1994)

ABSTRACT

A computer-based numerical model is presented, with which hydration and microstructural development in Portland cement-based materials can be simulated. The model, called HYMOSTRUC, the acronym for HYdration, MOrphology and STRUCtural development, enables the prediction of hydration curves as a function of the particle size distribution and chemical composition of the cement, the water/cement ratio and the actual reaction temperature. The influence of microstructural development, i.e. the formation of interparticle contacts, on the rate of hydration is modelled explicitly.

The background and structure of the simulation model are discussed in Part I of the series. Characteristic model features and the predictive potential of the model as regards the hydration process, hydration temperatures and microstructural development in both bulk cement paste and in the matrix-aggregate interfacial zone will be dealt with in Part II. A detailed explanation of the model is found in (2).

Introduction

Quality control on the building site is one of the major challenges in engineering practice in our days. In this framework computer programs have been developed for analyzing the risk of early-age thermal cracking in concrete structures. The input for most of these "macro-level programs" consists of, among other things, either an adiabatic, an isothermal or a semi-adiabatic hydration curve of the concrete mix. There is in increasing demand for predictive models with which these curves can be generated numerically. For this purpose a numerical model has been developed with which the engineer's wishes can be fulfilled to a large extent and which is, moreover, as consistent as possible with present views on processes and mechanisms involved in hydration and microstructural development.

Main Characteristics Of Existing (Numerical) Models

Hardening of cement-based materials is affected by at least four parameters, viz. the chemical composition and particle size distribution of the cement, the reaction temperature and the w/c ratio. The effect of each of these parameters on the rate of hydration has been investigated thoroughly in the past by researchers from different disciplines: cement chemistry, stereology and granulometry, physics and colloid chemistry.

Among the chemistry-oriented models are the Avrami-Erofeev and Kolmogoroff-Erofeev models. In those models the effect of the particle size distribution and the development of interparticle contacts on the rate of hydration are allowed for implicitly in the experimental formula constants of the model.

The importance of the particle size distribution of the cement on the rate of hydration has been emphasized in classical papers of Kondo et al. (9), Taplin (10) and, later, Bezjak (3) and Knudsen (11). As regards the type of reaction the first authors distinguished between, among other things, boundary and diffusion controlled reactions. In the diffusion layer, formed by the reaction products, there was distinguished both *inner* and *outer* product with different diffusion coefficients. Pommersheim (13) furthermore considered an *intermediate* layer, which would gradually disappear with increasing degree of hydration. A decrease of the diffusion coefficient with increasing degree of hydration, as observed in many tests, has been ascribed to densification of the gel due to merging of hydration products when formed in an increasingly confined space (22).

Parrott (14) has suggested approximating the rate of reaction of a poly-mineral material like cement by adding the separate contributions of the individual components, assuming that these components hydrate independently. Although good results with this model have been reported it can not be denied that in a number of experiments at least some interaction between hydration compounds has been observed (15,20). The truth seems to be somewhere between the two extremes formed by the "independent hydration concept" as proposed by Parrott on the one hand, and the "equal fractional rates concept" as supported by Brownmiller (15), Rexford (34) and others on the other hand (for a survey, see (2)).

In those models microstructural development and its effect on the rate of hydration are not considered explicitly. Explicit modelling of interferences between processes, mechanisms and reactions involved in the hardening of a poly-size and poly-mineral cement-water system is, in essence, a prerequisite for consistent modelling and is certainly one of the most intricate challenges of computational materials science. Frohnsdorff (16) was among the first who outlined the structure of a numerical model, with which hydration and microstructural development of a cement paste could be simulated more or less comprehensively. The potential of modern computers to simulate the complex and mutually interrelated processes and mechanisms occurring in hardening cement based materials have been emphasized more recently by Jennings (17). Recent work of Bentz and Garboczi (1,18) is a good example of the computer-based approach on a fundamental level.

Objectives Of The Study

A major objective of the present study was to develop a model with which *hydration* and *microstructural development* in a hardening cement paste could be simulated as two interrelated phenomena. In the model allowance should be made for the effect of the *chemical composition,* the *particle size distribution* of the cement, the *w/c ratio* and the *temperature regime*. Explicit modelling of microstructural development should illuminate mechanisms and parameters involved in strength development.

In view of the desired applicability of the model in engineering practice, the computation time required for one single simulation should not exceed what is considered reasonable within the stringent time schedules normal to engineering practice.

Bearing in mind the complexity of the subject and in order to end up with a workable model, rigorous systematization will be required to describe the predominant characteristics of the cement itself, of the hydration products and of the mechanisms and processes involved in hydration and structural development. In order to be able to implement additional options in the model in later stages without drastic restructuring of the model, the structure of the model should be as "open" as possible (see also Jennings (17)).

Model For Hydration And Microstructural Development

Background considerations and assumptions

In the model the development of microstructure is considered as a process of formation of contacts between expanding cement particles. Expansion occurs because the volume of the reaction products exceeds the volume of the dissolving reactant by a factor v, i.e. $v \cong 2.2$. For numerical simulation of the formation of interparticle contacts it is assumed that:

1. Reaction products are formed close to dissolving cement grains (6);
2. The density of the reaction product (gel) in case of isothermal curing is constant throughout the hydration process and independent of the place where it is formed. The effect of the curing at elevated temperatures on the (capillary) pore structure and density is modelled explicitly.
3. Both dissolution and expansion of the cement particles occur concentrically. The rate at which the reaction front proceeds into an anhydrous cement grain is expected to be a function of the chemical composition of the cement.
4. Particles of the same size hydrate at the same rate.
5. Cement components are considered to hydrate at equal fractional rates. In a later stage of development of the model the effect of physio-chemical interactions between different hydrating constituents on the rate of reaction has to be considered in more detailed.

With progress of the hydration process small particles, located in the close vicinity of bigger particles, will gradually become engulfed by, and embedded in, the outer shell of the latter. The effect of embedding particles in the outer shell of expanding particles on the rate of hydration is at least two-fold. Firstly, embedding of particles causes an extra increase of the product layer and will, therefore, cause a decrease of the rate at which ions can diffuse from the aqueous phase to the anhydrous cement core and vice versa. Secondly, embedded particles, which are not fully hydrated at the moment when they become engulfed, will continue to hydrate while withdrawing a certain amount of water from the particle in the outer shell of which they are embedded, thus reducing the rate of hydration of the latter particle. Particles and clusters of particles, which are not embedded in the outer shell of bigger particles, are identified as *free* particles and *free* clusters.

For quantification of the interaction process described, the *stereological aspect* of microstructural development is of paramount importance and necessitates considering both the particle size distribution and the spatial distribution of the cement particles in the paste.

Stereological aspects of particle interaction

For the particle size distribution of the cement the well-known Rosin-Ramler distribution:

$$G(x) = 1 - \exp(-bx^{n}) \qquad (1)$$

has been adopted, with x [µm] the particle diameter and b and n constants which are determined so that $G(x \rightarrow \infty) = 1$ gram. The particles are assumed to be spherical. It has to be born in mind that the assumption of sphericallity of cement particles affects the interpretation of hydration data. The rate of penetration of a reaction front found by back-calculation from the degree of hydration will be higher for spherical particles than for non-spherical particles (2,23).

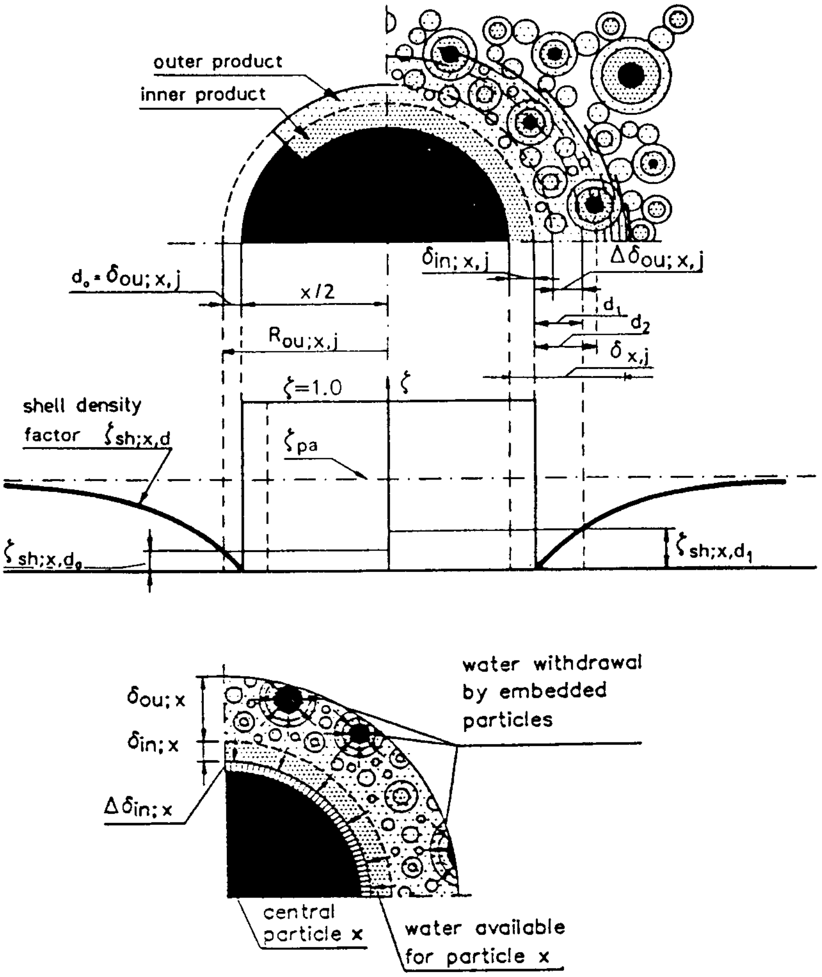

Fig. 1a

Fig. 1b

FIG. 1

Schematic representation of expansion mechanism and water withdrawal (2).

a. Upper part - Left: No embedding of particles
   Upper part - Right: Enhanced expansion caused by embedding of neighbouring particles
   Bottom part: Shell density curves $\zeta_{sh;x,d}$
b. Water withdrawal mechanism: schematic

In reality the cement particles will be randomly distributed in the paste. Since each particle has, therefore, a unique position in the system, the formation of interparticle contacts, as well as the effect of these contacts on the hydration kinetics of each particle, will be different for each individual particle. If we would decide to follow the hydration process of each individual particle explicitly, the computation times required for a simulation of a representative polysize sample would soon exceed the capacity of present generation personal computers (which was considered a prerequisite). The computation time is reduced dramatically by postulating that particles of the same size hydrate at the same rate, so that the mean rate of hydration is computed. This is, in fact, the rate of hydration of interest in engineering practice.

In the calculation procedure the cement particles are first assumed to be equally spaced in the paste. An arbitrary particle x is considered to be located in the centre of a "cell", and is called the "central particle". For this homogeneous distribution of the cement particles it is relatively easy to determine the *amount of cement* present in a *fictitious shell* around an arbitrary central particle x. For the purpose a *shell density factor* $\zeta_{sh;x,d}$ is defined:

$$\zeta_{sh;x,d} = \frac{\text{amount of cement } [\mu m^3] \text{ in a spherical shell with thickness d}}{\text{total volume } [\mu m^3] \text{ of the shell}} \tag{2}$$

For a particular paste the course of the shell density factor belonging to a particle with diameter x is shown schematically in the bottom part of Fig. 1a. Going from the periphery of the central particle x in the outward direction the shell density gradually increases from zero at the surface of the central particle to the bulk density $\zeta_{pa} = [1+\omega_0 * \rho_{ce}]^{-1}$, in which ω_0 is the w/c ratio and ρ_{ce} the specific mass of the cement.

In order to allow for the actual randomness of the particle distribution it is assumed in further numerical evaluations that the cement present in a fictitious shell around a central particle x consists of particles with diameters < x μm. A consequence of the chosen procedure is that the *number* of particles involved in the interaction process must be counted carefully in order not to count them more than once (for additional details, see (2)).

Particle expansion mechanism. Basic structure of the algorithm

An arbitrary stage in the hydration process of a central particle of diameter x is shown schematically in the upper part of Fig. 1a. At a certain time, say t_j, the degree of hydration of the particle is $\alpha_{x;j}$. For the corresponding *penetration depth* $\delta_{in;x,j}$ of the reaction front it holds:

$$\delta_{in;x,j} = \frac{x}{2} * [1 - \{1-\alpha_{x,j}\}^{\frac{1}{3}}] \tag{3}$$

The volume of outer product that corresponds with the degree of hydration $\alpha_{x;j}$ of particle x follows from:

$$v_{ou;x,j} = (\nu-1) * \alpha_{x,j} * v_x \tag{4}$$

with v_x the volume of particle x in its anhydrous state. If no cement would be found in the spherical outer shell which is filled up with outer product of the expanding particle (Fig. 1a, upper-left), the outer radius $R_{ou;x,j}$ of particle x would be:

$$R_{ou;x,j} = [\frac{v_{ou;x,j}}{4\pi/3} + (\frac{x}{2})^3]^{\frac{1}{3}} \tag{5}$$

For the thickness $\delta_{ou;x,j}$ of the outer shell it would follow:

$$\delta_{ou;x,j} = R_{ou;x,j} - \frac{x}{2} \tag{6}$$

In reality a certain amount of cement will be present in the outer shell. The volume of the cement in a shell with thickness $\delta_{ou;x,j}$, called the *directly embedded cement volume* $v_{em;x,j}$, is determined by multiplying the shell volume $v_{ou;x,j}$ by the corresponding shell density factor $\zeta_{ou;x,d_0}$ (with $d_0 = \delta_{ou;x,j}$):

$$v_{em;x,j} = \zeta_{sh;x,d_0} * v_{ou;x,j} \tag{7}$$

The volume of the embedded, partly hydrated, cement accounts for an additional expansion $\Delta\delta_{ou;x,j}$ of the outer shell of particle x. In turn this additional expansion results in an increase of the amount of embedded cement. The volume of cement found in the shell with a thickness $\Delta\delta_{ou;x,j}$ is called the *indirectly embedded cement volume.* The total volume of directly and indirectly embedded cement can be calculated analogously to the procedure for the determination of the directly embedded cement (formulae (2) and (7)), albeit that the shell density factor is a little higher because of the increase of the thickness of the outer shell (Fig. 1a, bottom part: $\zeta_{sh;x,d_1} > \zeta_{sh;x,d_0}$). The increase in the amount of embedded cement causes another additional increase in thickness of the outer shell and the process is repeated. This expansion mechanism can be written in the form of a geometrical series. Numerical evaluation results in workable expressions for the thickness of the outer shell of particle x and for the total thickness of the layer of reaction products at time t_j, viz. $\delta_{x,j}$, as well as for the amount of cement embedded in the outer shell of particle x. Adding the amounts of cement embedded in the outer shells of all free particles in the system yields the amount of cement involved in the interaction process at time t_j.

Rate of penetration of the reaction front

The rate of penetration of the reaction front in an individual cement particle x at time t_j is computed with a *basic rate formula* (written in a reduced form):

$$\frac{\Delta\delta_{in;x,j+1}}{\Delta t_{j+1}} = K_0(.)*\Omega_1(.)*\Omega_2(.)*\Omega_3(.)*F_1(.) * \left[F_2(.) * \left(\frac{\delta_{tr}(.)}{\delta_{x,j}}\right)^{\beta_1} \right]^{\lambda} \tag{8}$$

with $\Delta\delta_{in;x,j+1}$ the increase of the penetration depth in time step Δt_{j+1}, $K_0(.)$ the *basic rate factor* [μm/h], $\delta_{tr}(.)$ the *transition thickness* [μm], being the total thickness of the product layer $\delta_{x,j}$ at which the reaction for the particle in view changes from a *boundary reaction* ($\lambda = 0$) into a *diffusion controlled reaction* ($\lambda = 1$). The thickness, at which this change will take place, depends on the type of cement and has been determined by evaluating hydration data obtained with different Portland cements. β_1 is an empirical constant.

The first five factors on the right-hand part of eq. (8) are operational during both the boundary reaction and the diffusion controlled stage of hydration, whereas the term in straight brackets is only operational in the diffusion controlled stage. The value of the term in straight brackets has been determined so that the rate of penetration of the reaction front immediately before and after the change from a phase-boundary reaction to a diffusion controlled reaction is the same.

Boundary reaction

The basic rate factor $K_0(.)$ is assumed to be a function of the chemical composition of the cement and has to be determined from an evaluation of hydration tests. The $\Omega_i(.)$-factors (i = 1,2,3) allow for the state of water in the pore system of the hardening paste. The $F_i(.)$-factor (i = 1) accounts for the effect of temperature on the rate of reaction.

The factor $\Omega_1(.) = \Omega_1(x,\alpha_{x,j})$ accounts for the effect of *water withdrawal* by the embedded and still hydrating particles on the rate of penetration of the reaction front in particle x. The water withdrawal mechanism is shown schematically in Fig. 1b. For three particle sizes, viz. x = 20, 40 and 110 µm, the reduction factors $\Omega_1(.)$ are given in Fig. 2 for a paste with $\omega_0 = 0.4$. For low w/c ratios the reduction factors for large particles may approach zero because most of water needed for further hydration is consumed by embedded small particles.

The factor $\Omega_2(.) = \Omega_2(\alpha)$ allows for the effect of the *distribution* of the water in the pore system of the paste. The water in the paste is concentrated in the smaller pores, whereas larger pores are gradually emptied. The absence of water in the larger pores causes a reduction of the rate at which the cement immediately adjacent to the walls of the empty pores can hydrate, thus reducing the overall rate of hydration. For quantifying this "empty pore effect" the following formula has been derived (2):

$$\Omega_2(\alpha) = \frac{\phi_{wat;\alpha} - \phi_0}{\phi_{por;\alpha} - \phi_0} * \frac{\phi_{por;\alpha}}{\phi_{wat;\alpha}} \tag{9}$$

in which $\phi_{wat;\alpha}$ and $\phi_{por;\alpha}$ are the pore diameters of the largest capillary pore which is still completely filled with water and the largest capillary pore in the paste as a whole, respectively.

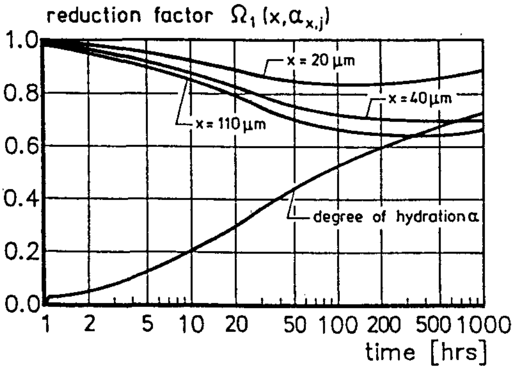

FIG. 2

Reduction factor $\Omega_1(x,\alpha_{x,j})$ accounting for water withdrawal by embedded particles (α = overall degree of hydration) (2).

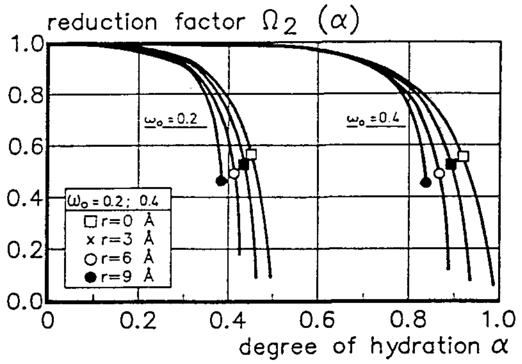

FIG. 3

Reduction factor $\Omega_2(\alpha)$ as a function of the degree of hydration. Thickness of adsorption layer as parameter (2).

ϕ_0 is the (minimum) characteristic size of gel pores as proposed by Powers (28), i.e. ϕ_0 = 20 Å. Formula (9) represents the ratio between the capillary pore wall area in contact with water and the total capillary pore wall area. For the pore size distribution and changes of it with progress of the hydration process experimental data (mercury intrusion) of Whiting et al. (29) were used. By definition these experimental data of pore size distribution depends on the adopted measuring method. As a consequence of this the factor $\Omega_2(\alpha)$ gives a *trend* and enables the performance of sensitivity studies regarding the effect in view. Indicative values for $\Omega_2(\alpha)$ are shown in Fig. 3 for pastes with $\omega_0 = 0.2$ and $\omega_0 = 0.4$. The curves in this figure are obtained for different thicknesses Γ [Å] of the water layer adsorbed at the walls of the empty pores. Thickness is a function of the relative humidity in the pore system. For a three monomolecular water layer with a thickness of about 9 Å the ultimate degree of hydration in the paste with $\omega_0 = 0.4$ would not exceed 85%. According to Hagymassy (30) a three monomolecular layer is stable at a relative humidity RH ≈ 80%. Work of Parrott et al. (31) shows that hydration almost ceases when the relative humidity drops to below about 80% (see Fig. 4). This result appears to agree broadly with the cessation of hydration as predicted with the factor $\Omega_2(\alpha)$.

Besides the *distribution* of the water the *amount* of water also affects the rate of hydration. For hydration of C_3S Damidot et al. (32) concluded that the lower the amount of water the smaller the rate of dissolution. Against the background of his result is was assumed that the gradually decreasing amount of water is a factor in the *dynamic equilibrium* of a process of dissolution of anhydrous cement and precipitation of reaction products. For the effect of the decreasing amount of water on the overall rate of hydration a reduction factor $\Omega_3(\alpha)$ is postulated (2):

$$\Omega_3(\alpha) = \frac{\omega_0 - 0.4\,\alpha}{\omega_0} \qquad (10)$$

According to this reduction factor the overall rate of hydration reduces proportionally with the amount of capillary water. A similar correlation between the rate of hydration and the capillary pore water has been suggested by Röhling et al. (33). For further justification of this reduction factor additional research is required. In this research due attention has to be given to the fact, that almost simultaneously with the decrease of the amount of water in the paste a significant change in the ion concentration occurs. This change starts at the beginning of the acceleration period, when the degree of hydration is still rather low [19]. Whether this change is the cause or the results of a lower rate of hydration, and what role the amount of water plays is still a point of discussion. More information on interrelated phenomena, processes and mechanisms involved in this stage of hardening is certainly needed.

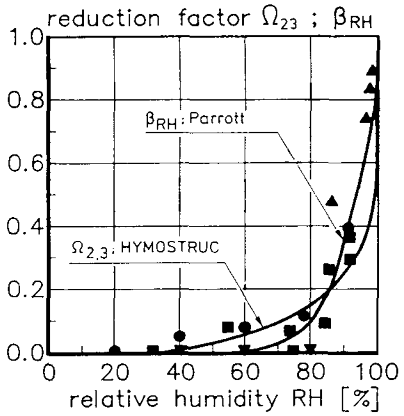

FIG. 4
Effect of relative humidity on the rate of hydration. Experimental data indicated with discrete points (2).

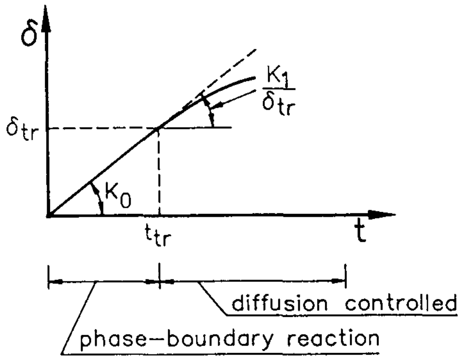

FIG. 5
Relationship between basic rate factor $K_0(.)$, diffusion coefficient $K_1(.)$ and transition thickness $\delta_{tr}(.)$. Schematic.

Literature data (21,24) on the relationship between the development of the pore size distribution in a hydrating paste and thermodynamically determined relationships between the amount and distribution of pore water in a given pore system and the relative humidity in the empty pores, enable us to correlate the degree of hydration with the relative humidity in the pore system

(2). The correlation between the degree of hydration and the relative humidity being known for a particular mix, the combination factor $\Omega_{23}(\alpha) = \Omega_2(\alpha)*\Omega_3(\alpha)$ can be presented as a function of the relative humidity RH. This enables us to compare the combination factor $\Omega_{23}(RH)$ with a similar reduction factor β_{RH} proposed by Parrott (14). As shown in Fig. 4, the Ω_{23}-RH relationship is in good agreement with the reduction factor proposed by Parrott and the experimental presented by him.

The effect of temperature on the rate of reaction is accounted for with the function $F_1(.)$ according to the Arrhenius function:

$$F_1\{T,\alpha,C_3S\} = A * e^{-\frac{AE\{T,\alpha,C_3S\}}{R*(273+T)}} \qquad (11)$$

in which R is the gas constant (8.31 J/mol K) and AE the apparent activation energy. The latter quantity was found to be an empirical function of the actual values of the degree of hydration α, the curing temperature T and the chemical composition of the cement, ergo the C_3S content (2). From an evaluation of experimental data published by Lerch et al. (8) the following expression for the apparent activation energy EA was obtained:

$$AE\{T,\alpha,C_3S\} = p_0 * \alpha * e^{-[m*(C_3S\%)^n+0.025*T^{\frac{3}{2}}]} + 0.33*(C_3S\%) + 30 \qquad (12)$$

with m = 2.52 10^{-11} and n = 6.15 (2). For the constant A in eq. (11) it holds:

$$A = e^{\frac{AE(T_{20})}{R*293}} \qquad (13)$$

in which $AE(T_{20})$ is the apparent activation energy for T = 20°C. The fact that the apparent activation energy appears to be function of temperature demonstrates that this quantity can not be considered as an activation energy in the proper sense of the word. The temperature dependency of this empirical quantity is assumed to be attributable to temperature dependent changes in the microstructure.

Diffusion controlled stage

When the thickness of the product layer has reached the transition thickness $\delta_{tr}(.)$, the term in straight brackets on the right-hand part of eq. (8) becomes operational ($\lambda = 1$). In this stage the rate of penetration in particle x is inversely proportional to the β_1-power of the thickness of the product layer $\delta = \delta_{x,j}$ at time t_j. For a smooth change from the boundary reaction into the diffusion controlled reaction the following relationship between the basic rate factor $K_0(.)$ and the coefficient of diffusion $K_1(.)$ [$\mu m^2/h$] is proposed (see also Fig. 5):

$$K_1(.) = K_0(.) * \delta_{tr}^{\beta_1} \qquad (14)$$

By writing the diffusion coefficient $K_1(.)$ as the product of the basic rate factor $K_0(.)$ and the transition thickness $\delta_{tr}(.)$, the determination of the diffusion coefficient has been brought back to the determination of the transition thickness, supposing that the basic rate factor is known already from a detailed evaluation of hydration kinetics in the stage when the phase-boundary reaction was rate controlling.

In the case of isothermal curing the diffusion resistance of the gel is assumed to be a constant throughout the hydration process. An increase of diffusion resistance with elapsed time as suggested by several authors (Pommersheim et al. (25)), and which has been ascribed to densification of the gel due to the development of interparticle contacts, was *not* considered since the effect of the development of interparticle contacts is allowed for *explicitly* in the present model.

Experimental data on the relationship between capillary porosity and curing temperature shows an increase in capillary porosity with increasing temperature (26,27). This has been ascribed to densification of the hydration products and a corresponding reduction of the porosity of the calcium silicate hydrates with increasing curing temperature above 20°C (38). A temperature function $F_2(.)$ is introduced to allow for this temperature-related densification of the hydration products on the rate of hydration. From experimental data of Bentur et al. (26) on the effect of temperature on the capillary pore structure on C_3S pastes the following expression for the temperature dependency of the density of hydration products has been derived (valid in the temperature range from $0°C < T < 60°C$) (2):

$$\nu(T) = 2.22 * e^{-28\ 10^{-6} * T^2} \tag{15}$$

In this expression the temperature T is a constant. In case of a variable curing temperature, as is the normal case in engineering practice, a "weighted temperature $\bar{T}$", i.e. the mean temperature in the *hydration domain*, is adopted according to:

$$\bar{T}_j = \frac{1}{\alpha_j} * \int_0^{\alpha_j} T(\alpha)d(\alpha) \tag{16}$$

The temperature-caused densification of the diffusion layer is assumed to cause an increase of the diffusion resistance and hence a reduction of the rate of penetration of the reaction front (36). In the absence of quantitative data on the effect of densification of the reaction products on the rate of penetration of the reaction front a reduction factor was adopted according to:

$$F_2(T) = \left(\frac{\nu(T)}{\nu_{20}} \right)^{\beta_2} \tag{17}$$

in which $\nu_{20} = \nu(T_{20}) = 2.2$. β_2 is an empirical constant.

The temperature dependency of the density of the hydration products will *also* affect the magnitude of the transition thickness $\delta_{tr}(.)$. Temperature-induced densification of the products layer is assumed to cause a reduction of the transition thickness according to:

$$\delta_{tr}(T) = \delta_{tr,20} * \left(\frac{\nu(T)}{\nu_{20}} \right)^{\beta_2} \tag{18}$$

in which $\delta_{tr,20}$ is the transition thickness for isothermal hydration at T = 20°C. In its final form the term in straight brackets in eq. 8 reduces to (2):

$$\left[F_2(.) * \left(\frac{\delta_{tr}}{\delta_{x,j}}\right)^{\beta_1}\right]^{\lambda} = \left[\left(\frac{\nu(\bar{T}_j)}{\nu_{tr}(\bar{T}_j)}\right)^{\beta_2} * \left\{\left(\frac{\nu(\bar{T}_j)}{\nu_{20}}\right)^{\beta_2} * \left(\frac{\delta_{tr,20}}{\delta_{x,j}}\right)\right\}^{\beta_1}\right]^{\lambda} \tag{19}$$

Using this relation the rate of penetration of the reaction front in a cement particle with diameter x can be determined from eq. (8). From the penetration depth the amount of cement that has reacted can be computed. The overall degree of hydration of a poly-size sample is found by adding the amounts of the cement of all the cement particles in the system.

In the basic rate formula (8) the effect of the particle size distribution, the w/c factor and the temperature are now allowed for explicitly. The model parameters $K_0(.)$, $\delta_{tr}(.)$, β_1 and β_2 are functions of the chemical composition of the cement.

Model Parameters

For the determination of the model parameters $K_0(.)$, $\delta_{tr}(.)$, β_1 and β_2 an evaluation program was conducted. In this program over 60 hydration tests were involved, comprising 27 different types of Portland cement with C_3S contents ranging from 15% to 70%. The w/c ratios varied from 0.16 to 0.8, particle size distributions with n-values (eq. (1)) ranging from 0.73 to 3.15 and curing temperatures from 4°C to over 50°C. The model parameters were determined so as to achieve a satisfactory fit of calculated hydration curves with the experimental data (a discrepancy between experimental data and simulations of 10...15% on the average was considered satisfactory).

The $K_0(.)$-values were written as a function of the C_3S content:

$$K_0(C_3S) = 0.02 + 6.6\ 10^{-6} * [C_3S\%]^2 \qquad [\mu m/h] \qquad (20)$$

with a standard deviation $\sigma(K_0) = 0.008$ μm/hr. Attempts to correlate the $K_0(.)$-value to the C_3A-content or to a combination of the C_3S and C_3A content resulted in a higher standard deviation. For this reason it was decided to concentrate in this stage of the project on the correlation with the C_3S-content.

The basic rate factor $K_0(C_3S)$ is the *only* model parameter which influences the rate of reaction in the early boundary reaction stage of the hydration process. Hence, its value is not affected by the values of the three remaining model parameters which become operational in the diffusion controlled stage of the process (eq. (8), with $\lambda = 1$).

The transition thickness $\delta_{tr}(.)$ appeared to be weakly correlated with the C_2S content:

$$\delta_{tr}(C_2S) = -\ 0.02 * [C_2S\%] + 4 \qquad [\mu m] \qquad (21)$$

For a low-heat cement values ranged from 2 to 4 μm. For rapid hardening cements values from 3 to 6 μm were found. These values are in rather good agreement with those deduced from the experimental work of Bezjak et al. (3) and Alujevic et al. (4). For the ratio between rate factors more or less comparable with the $K_1(.)$ and $K_0(.)$ defined in preceding sections, they found values from 1.7 to 3.4. For the time being the data of Bezjak and Alujevic is the only source for checking the values of the transition thickness. For further justification more research is needed.

For the factors β_1 and β_2 a value of 2 was applicable in the majority of cases. Variations in these factors in the range from 1 to 2 predict variations in the 28-days hydration values of about 5% to 10%. Variations of the same order of magnitude can be ascribed to the gypsum content and the alkali content (2,35). Since the effects of gypsum and minor constituents are not accounted for explicitly in the model yet, attempts to correlate the β-values to the chemical composition of the cement are not warranted.

Discussion

In the model presented in this paper emphasis is on the stereological aspects of hydration and microstructural development. Less attention was paid to the chemistry-oriented aspects. Future work shall concentrate on a more realistic description and modelling of the chemical aspect, for example along the lines outlined in the work of Parrott et al. (14) and Osbeack (37). In the present stage of development of the model the chemical aspect is allowed for in the empirical factors $K_0(.)$, $\delta_{tr}(.)$, β_1 and β_2 in the basic rate equation (8). With regard to these factors the following preliminary comments are made. The $K_0(.)$- and $\delta_{tr}(.)$-values vary little with variations in the β-values. Only a weak correlation exists between the β-values and the chemical composition of the cement. Thus the effect of the chemical composition of the cement can be described by mainly two factors (at least in this model), viz., the basic rate factor $K_0(C_3S)$ and the transition thickness $\delta_{tr}(C_2S)$.

If not specified otherwise, the simulation program HYMOSTRUC operates with the *default values* for the model parameters $K_0(C_3S)$ and $\delta_{tr}(C_2S)$ provided by the eqns. (20) and (21), respectively, and with values $\beta_1 = 2$ and $\beta_2 = 2$.

Characteristic model features and the predictive potential of the model are presented in a second part of this paper.

References

1. E.J. Garboczi, D.P. Bentz, 9th Int. Congr. Chem. Cem., New Delhi, Vol. VI, 3 (1992).
2. K. van Breugel, Simulation of Hydration and Formation of Structure in Hardening Cement-Based Materials, p. 295, W.D. Meinema, (1991).
3. A. Bezjak, I. Jelenic, Cem. Concr. Res., 10, 553 (1980).
4. V. Alujevic, et al., Cem. Concr. Res., 16, 695 (1986).
5. K. Scrivener, A. Bentur, P.L. Pratt, Adv. Cem. Res., I, 230 (1988).
6. H.F.W. Taylor, D.E. Newbury, Cem. Concr. Res., 14, 565 (1984).
7. J.H. Taplin, Austr. Journ. Appl. Sci., 10, 329 (1959).
8. W. Lerch, C.L. Ford, Journ. Am. Concr. Inst., 44, 745 (1948).
9. R. Kondo, S. Ueda, 5th Int. Congr. Chem. Cem., Tokyo, II, Sess. II-4, 203 (1968).
10. J.H. Taplin, 5th Int. Congr. Chem. Cem., Tokyo, II, Sess. II, 249 (1968).
11. T. Knudsen, Cem. Concr. Res., 14, 622 (1984).
12. A. Bezjak, Cem. Concr. Res., 13, 305 (1983).
13. J.M. Pommersheim, 7th Int. Congr. Chem. Cem., Paris, Theme VI, 195 (1980).
14. L.J. Parrott, D.C. Killoh, "Prediction of cement hydration" in The chemistry and chemically-related properties of cement, Ed. D. Glasser, pp. 41-53, Brit. Cer. Soc., Shelton, 1984.
15. L.T. Brownmiller, Journ. Am. Concr. Inst., 14, 193 (1943).
16. G.J.C. Frohnsdorff, W.G. Freyer, P.D. Johnson, 5th Int. Congr. Chem. Cem., Tokyo, 2, 321 (1968).
17. H.M. Jennings, Symp. on Microstructural Development During Hardening of Cement, Boston, 85, 291 (1986).
18. D.P. Bentz, E.J. Garboczi, Cem. Concr. Res. 21, 325 (1991).
19. A.L.A. Fraay, A.L.A., Fly ash as a pozzolan in Concrete, Tech. Univ. Delft, PhD, 1990.
20. G. Yamaguchi, K. Takemoto, H. Uchikawa, S. Takagi, Zement-Kalk-Gips, 10, 467 (1990).
21. W. Grün, H.R. Grün, Zement-Kalk-Gips, 3, 514 (1961).
22. J.M. Pommersheim, J.M., Cem. Concr. Res. 12, 765 (1982).
23. Li Jian-Xi, , 9th Int. Congr. Chem. Cem., New Delhi, IV, 525 (1992).
24. M.J. Setzer, Deutscher Ausschuss für Stahlbeton, 280, Wilhelm Ernst & Sohn, Berlin, 280, 43 (1977).
25. J.M. Pommersheim, J.R. Clifton, Cem. Concr. Res., 9, 765 (1979).
26. A. Bentur, R.L. Berger, J.H. Kung, N.b. Milestone, J.F. Young, Journ. Am. Cer. Soc., 62, 362 (1979).
27. K.O. Kjellsen, R.J. Detwiler, O.E. Gjørv, Cem. Concr. Res., 21, 179 (1991).
28. T.C. Powers, T.L. Brownyard, Journ. Am. Concr. Inst., 18, 469 (1946).

29. D. Whiting, D.E. Kline, Cem. Concr. Res., 7, 53 (1977).
30. J. Hagymassy, S. Brunauer, R. Sh. Makhail, Journ. Coll. and Interface Sci., 29, 485 (1969).
31. L.J. Parrott, D.C. Killoh, R.G. Patel, 8th Int. Congr. Chem. Cem., Rio de Janeiro, II, 46 (1986).
32. D. Damidot, A. Nonat, in Hydration and Setting of Cements, p. 418, Ed. A. Nonat and J.C. Mutin, E & F Spon, London, 23 (1991).
33. S. Röhling, M. Nietner, A model to describe the kinetics of structure formation and strength development, Leipzig, p. 51, (1990).
34. E.P. Rexford, Journ. Am. Concr. Inst., 14, 212 (1943).
35. R.R. Keienburg, Kornverteilung und Normfestigkeit von Portlandzement, PhD, Aachen, p 111 (1976).
36. M. Laube, Werkstoffmodell zur Berechnung von Temperaturspannungen in massiggen Betonbauteilen im jungem Alter, PhD, Braunschweig, p. 251 (1990).
37. B. Osbeack, 9th Int. Congr. Chem. Cem., New Delhi, IV, 504 (1992).
38. L.J. Parrott, "Modelling of hydration reactions and concrete properties" in Materials science of concrete, Ed. J. Skalny, Am. Cer. Soc., 181 (1989).